

Structure optimization of *mixer ploughshare* through orthogonal experiment based on DEM simulation

Yaohua Zhu¹, Yan Li^{1,*} and Xinbo Chen²

¹School of Mechanical Engineering, Tongji University, China

²School of Automotive Studies, Tongji University, China

Abstract. In order to improve the mixing uniformity of plastic particles mixed by ploughshare mixer, the author extracted three structural parameters of the mixing structure and established nine models of orthogonal experiment. Use Discrete element method to simulate the mixing process of polypropylene and polyethylene particles, and take the coefficient of variation as the evaluation index of mixing uniformity. The experimental results showed that the optimal parameter combination is that the intersection angle of side blades is 40° , the circumferential distribution angle is 180° , and the axial distribution spacing is 164mm, when strength and abrasion resistance were verified as acceptable. The research method can provide certain reference for powder & particle material mixing analysis and equipment improvement.

Keywords: Ploughshare mixer, Orthogonal experiment, EDEM.

1 Introduction

As a new kind of efficient equipment for powder and particle mixing, ploughshare mixer is used in various occasions such as chemical industry, food, plastics, building materials, etc. In the ploughshare mixer, material diffusion and convection occur in three-dimensional space on the joint effect of ploughshares on the horizontal rotating shaft and lateral knives in container, so uniform mixing is achieved in a short time.

At present, relevant laws about material flow phenomenon and mixing quality control are mostly studied through equipment test in industrial field, while for theoretical research, simulation by discrete element method (DEM) becomes a feasible way. For example, through DEM simulation, Haoran Xu^[1] verified that the mixing effect of double screw across each other is better than that of double screw nesting. Ke Zhang^[2] studied the interaction between screw and concrete aggregate in screw conveyor based on the DEM-FEM coupling method, and put forward structure optimization opinions according to the numerical simulation results. As for mixing characteristics of ploughshare mixer, scholars have also done some research. B.F.C Larent^[3] verified the qualitative consistency

* Corresponding author: liyanliyan910@126.com

of the material flow pattern obtained by his DEM simulation and physical experiment at the speed of 2.25Hz. Paul W. Cleary^[4] compared the flow form and mixing behavior of particles under different recovery coefficients and friction coefficients with a single blade ploughshare mixer. Meysan Alian^[5] used lacey index as evaluation indicator of mixing uniformity to study the effects of rotating speed, container filling level and particle size on mixing.

In this paper, polypropylene and polyethylene in the plastic industry are taken as the mixed objects, three factor-three level orthogonal experiment is carried out via EDEM to optimize the structure and distribution parameters of a ploughshare, including intersection angle of side blades, circumferential distribution angle and axial distribution spacing.

2 Establishment of simulation model

2.1 The mixing structure

The mixing structure comes from a ploughshare mixer designed for 120L material volume and 20% filling level, whose modeling is shown in figure 1. Reducer's output shaft connecting the main shaft drives ploughshares to rotate around the horizontal axis, and several groups of rotary knives are arranged laterally in the cylindrical container to help break up agglomerated materials. Material is fed from the upper feed port and released from the bottom discharge port after mixing process is completed.

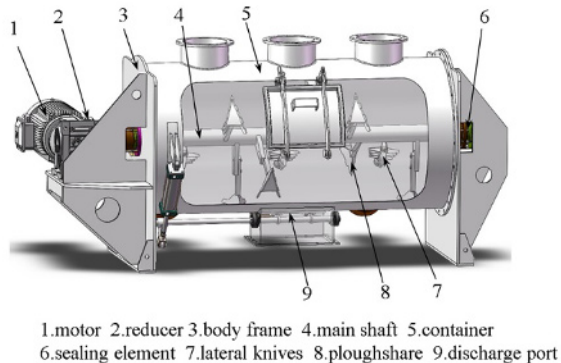


Fig. 1. The model of ploughshare mixer.

In order to facilitate the research, the assembly of ploughshare and main shaft refined. Ignoring the bolt connection, every ploughshare is integrated with its base to form a module. Thus, it is convenient to arrange the modules on the main shaft according to the distribution mode, which helps quickly construct the different mixing structures required by orthogonal experiment. The models of the main shaft and ploughshare are shown in figure 2.

2.2 Parameters to be studied

Intersection angle of side blades α , circumferential distribution angle β and axial distribution spacing p are adopted as the three factors of orthogonal experiment. Literature^[6-8] discusses the role of the ploughshare. Material not only moves in the circumferential direction, but also sprinkles outwards from both sides of the ploughshare by the action of ploughshare, resulting in crisscross motion tracks. Therefore, the intersection angle of the side blades has a certain influence on the mixing process.

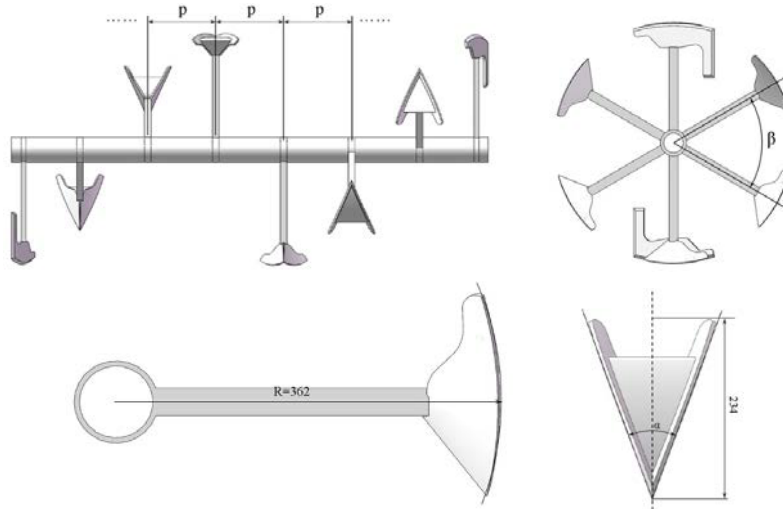


Fig. 2. The refined structure for mixing.

Ploughshares on the middle of the main shaft are arranged centrosymmetric, and then distributed along a spiral line to both sides. In this paper, the circumferential distribution angle between adjacent ploughshares is assumed same, which benefits the standardization of design and manufacture. Although Fang Z^[9] found that opposite distribution clamping 180° for ploughshares is possibly more conducive to the mixing performance, the ploughshares inserted into materials at the same time may suffer from greater resistance and wear. Therefore, it is worth studying the appropriate distribution angle. In addition, axial distribution spacing is also selected as one of the parameters to study.

In this paper, the values of each level of the three factors are shown in table 1. The value of axial distribution spacing p is obtained in turn by dividing the length of the main shaft by nine, seven and five.

Table 1. Factors and levels.

| Factors | Level-1 | Level-2 | Level-3 |
|----------|---------|---------|---------|
| α | 35° | 40° | 45° |
| β | 60° | 120° | 180° |
| p | 164mm | 210mm | 295mm |

2.3 Modeling of plastic particle

In the plastic industry, polypropylene (PP) and high-density polyethylene (HDPE) are often blended for modification. Firstly, the plastic particles are mixed with a high-speed mixer, and then extruded and granulated with a twin-screw extruder. Therefore, using the ploughshare mixer to mix plastic particles has practical significance.

According to relevant data, PP and HDPE's shear modulus, Poisson's ratio and density are valued as shown in table 2. The mixing structure and container are made of stainless steel, whose material parameters are also given below.

Table 2. Physical parameters of materials.

| Materials | Shear modules/MPa | Poisson's ratio | density/(kg/m ³) |
|---------------------|-------------------|-----------------|------------------------------|
| PP particle | 3.1e+8 | 0.42 | 900 |
| HDPE particle | 3.3e+8 | 0.38 | 950 |
| stainless steel 304 | 7.46e+10 | 0.30 | 7930 |

In this paper, real size of the prototype is used for modeling instead of scaling the prototype, thus, the mixing space in the container is relatively large. Made particle size be 15mm which is slightly larger than the real particle, so as to control the calculation scale and ensure the simulation accuracy. The particle shape adopts single sphere and the type of particle size distribution is ‘fixed’.

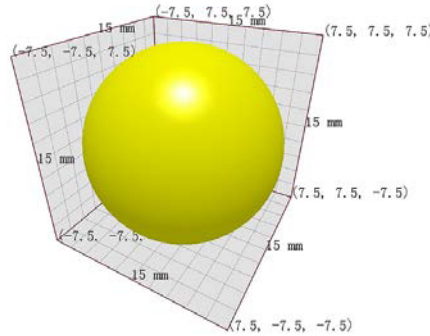


Fig. 3. Particle shape and size.

2.4 Principle of DEM

The discrete element method regards the analysis object as a sufficient number of elements, calculates the force and displacement of all elements in each time step according to the interaction between elements and Newton's law of motion, and updates the position of the elements by tracking their movement, so as to obtain the overall movement law of the analysis object^[10].

The soft-sphere model is employed in EDEM, whose collision process is non instantaneous. Besides the normal overlap, the tangential motion in the process of particle contact is divided into tangential sliding and rolling. The soft-sphere model is shown in figure 4.

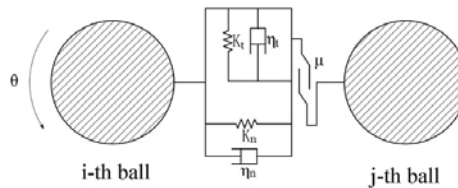


Fig. 4. Schematic diagram of soft-sphere model.

The differential equations of particle motion are as follows.

$$m_{1,2} \frac{d^2 u_n}{dt^2} + \eta_n \frac{du_n}{dt} + K_n u_n = F_n \tag{1}$$

$$m_{1,2} \frac{d^2 u_t}{dt^2} + \eta_t \frac{du_t}{dt} + K_t u_t = F_t \tag{2}$$

$$I_{1,2} \frac{d^2 \theta}{dt^2} + (\eta_t \frac{du_t}{dt} + K_t u_t) r = M \tag{3}$$

Where $m_{1,2}$ are the equivalent mass of particle, $I_{1,2}$ are the equivalent moment of inertia. u_n and u_t are the normal and tangential displacements of particle, and K_n and K_t are the normal and tangential stiffness coefficients, η_n and η_t are the normal and tangential damping coefficients. F_n and F_t are the normal and tangential components of the external force on the particle, and M is the external moment on the particle, θ is the particle's rotation angle and r is the rotation radius.

Since the actual bonding effect between plastic particles is so little that it could be ignored, the Hertz- Mindlin (no-slip) contact model is employed to describe the contact behavior. Therefore, the force and moment in the above equations are calculated according to the following formula.

$$F_n = \frac{4}{3} E^* \sqrt{R^*} \delta_n^{\frac{3}{2}} \tag{4}$$

$$F_t = 8G^* \sqrt{R^*} \delta_n \delta_t \tag{5}$$

$$M = \mu_r F_n R_i w_i \tag{6}$$

In the formula, E^* and G^* are equivalent Young's modulus and shear modulus respectively, and R^* is the equivalent radius of model particles, δ_n and δ_t are the normal overlap and tangential overlap. μ_r is the rolling friction coefficient, R_i is the distance from the particle centroid to the contact point, and w_i is the unit angular velocity vector of the particle at the contact point.

On the basis of existing literature and engineering experience of DEM simulation, the contact parameters of plastic and steel are taken according to table 3.

Table 3. Material contact parameters.

| Contact parameters | Value |
|--|-------|
| Plastic-plastic restitution coefficient | 0.45 |
| Plastic-steel restitution coefficient | 0.45 |
| Plastic-plastic static friction coefficient | 0.5 |
| Plastic-steel static friction coefficient | 0.5 |
| Plastic-plastic rolling friction coefficient | 0.05 |
| Plastic-steel rolling friction coefficient | 0.01 |

3 Simulation experiment

3.1 The design of orthogonal experiment

For the experimental conditions of three factors and three levels, L9 (34) orthogonal table is adopted in line with the theory of experiment design. L9(34) table is shown as table 4.

Import the models of container and ploughshare into EDEM in step format. The length of container is 1474mm and the inner diameter is 370mm. The distance from the top of the ploughshare to the rotation axis is 362mm. Set the rotation angular velocity of shaft and ploughshare at 62rpm by adding kinematic in line with the prototype.

Three particle factories are established at the three feed ports of the container, each of which is set to generate 6000 PP particles and 6000 HDPE particles in turn within 0.5s,

while the mixing structure just begins to rotate at the moment of 0.5s. The nine groups of mixing structures in the orthogonal experiment are shown in figure 5.

Table 4. Orthogonal table.

| Serial number | α | β | p |
|---------------|----------|---------|----------|
| 1 | 1(35°) | 1(60°) | 1(164mm) |
| 2 | 1(35°) | 2(120°) | 3(295mm) |
| 3 | 1(35°) | 3(180°) | 2(210mm) |
| 4 | 2(40°) | 1(60°) | 3(295mm) |
| 5 | 2(40°) | 2(120°) | 2(210mm) |
| 6 | 2(40°) | 3(180°) | 1(164mm) |
| 7 | 3(45°) | 1(60°) | 2(210mm) |
| 8 | 3(45°) | 2(120°) | 1(164mm) |
| 9 | 3(45°) | 3(180°) | 3(295mm) |

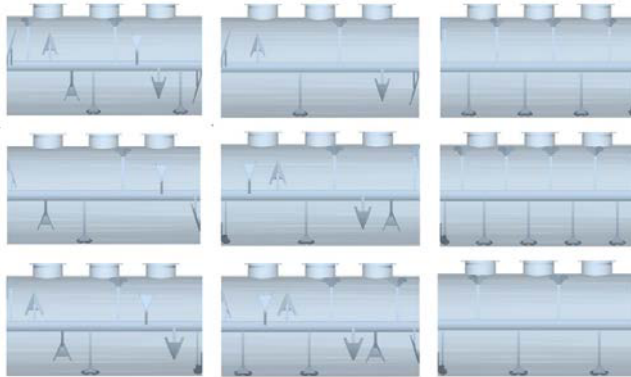
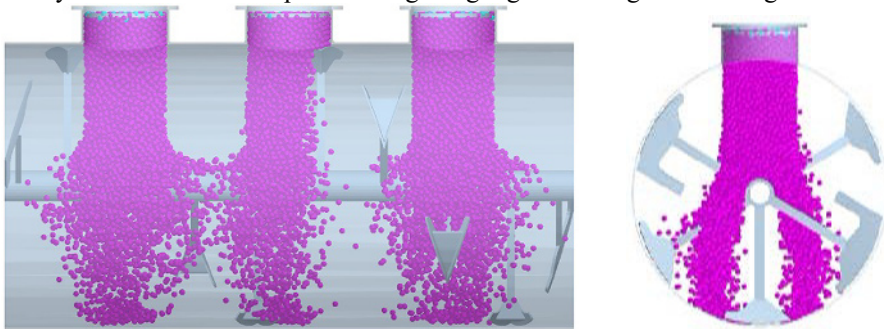


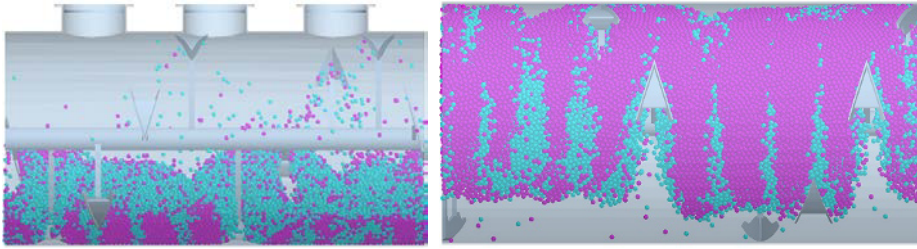
Fig. 5. Nine mixing structures.

3.2 Verification of the mixing mechanism

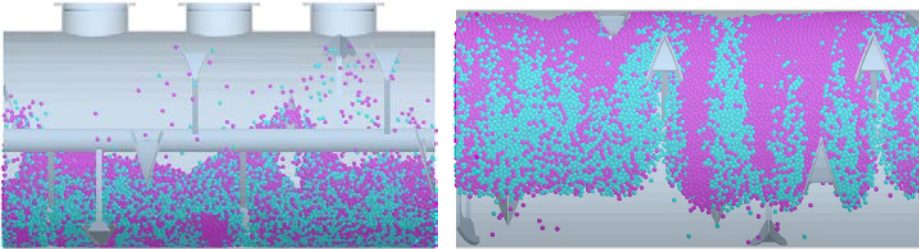
Set the simulation step as 0.02s and the total simulation time as 8s. After the simulation calculation is completed, PP particles and HDPE particles are colored and displayed respectively as magenta and cyan. Taking Exp. 1 as an example, the snapshots at 0.26s (when PP particles basically finish being generated and HDPE particles start to appear) and 2s, 4s, 6s and 8s are displayed in figure 6. From the figure, it is obvious that mixing uniformity of the two kinds of particles is getting higher and higher as time goes on.



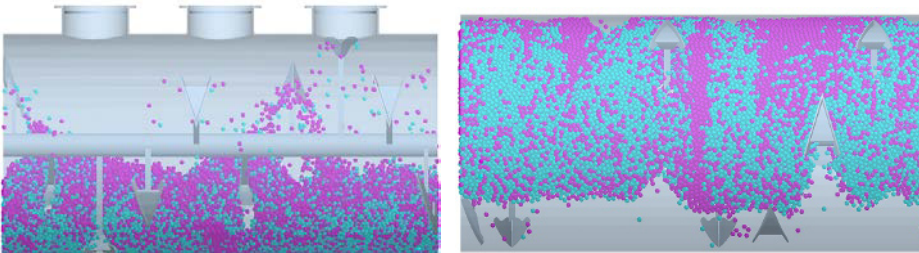
6(a) Snapshot at 0.26s.



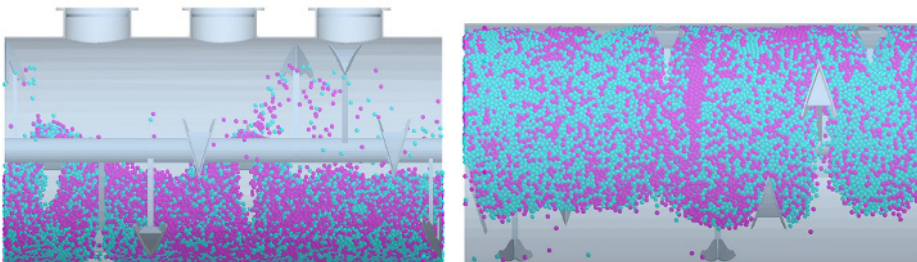
6(b) Snapshot at 2s.



6(c) Snapshot at 4s.



6(d) Snapshot at 6s.



6(e) Snapshot at 8s.

Fig. 6. Mixing process of Exp. 1.

In order to observe the particles' direction of motion, display the particles in the form of vector arrows. At 8s, a local snapshot in the mixer is shown in figure 7. It is visible that near the side blades of ploughshare, the particles are almost outward along the normal of the blades. Between adjacent ploughshares there is obvious material convective mixing. After material is pushed away by the blades, a temporary groove appears at the tail of the ploughshare, which is then filled by nearby material, forming a circumferential circulation of material.

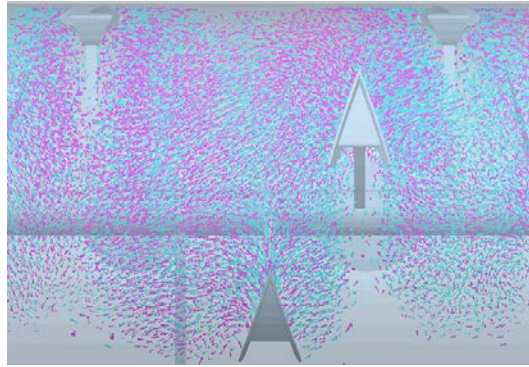


Fig. 7. Effect of ploughshares on particles.

4 Analysis of mixing uniformity

4.1 Grid creation and calculation of variation coefficient

Use the variation coefficient to quantitatively evaluate material mixing uniformity in the simulation experiment. The smaller the variation coefficient, the higher mixing uniformity.

Taking Exp. 1 as an instance, the materials are mainly distributed at one side of the bottom rather than the middle area under the influence of mixing, gravity and inertia, as shown in figure 8. Divide the material-existing area into $10 \times 3 \times 8$ grids, and select those grids as samples whose address meets that x equals to 1 ~ 10, y equals to 1 and z equals to 4-5; Or x equals to 1 ~ 10, y equals to 2 and z equals to 2~7, covering a total of 80 grids. Because these grids are almost completely occupied by material particles and would not become empty due to the dynamic flow of materials. Therefore, it is more scientific and reasonable using them as samples to calculate the coefficient of variation, which overcomes the deficiency that the evaluation of mixing uniformity by using variation coefficient is easy to be affected by local grids as described in reference^[11].

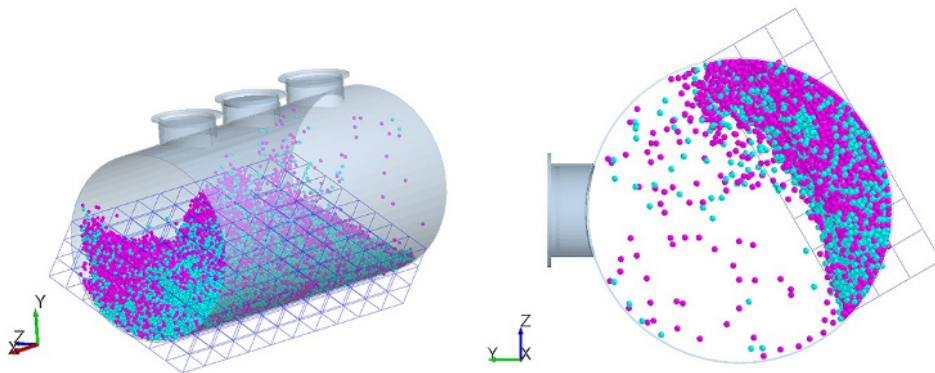


Fig. 8. The grids.

Taking HDPE particle as an example, the coefficient of variation is calculated according to the following mathematical model^[12].

Take M samples from the mixed region. If the total number of particles in each sample is N_i and the number of HDPE particles is n_i , then the proportion of HDPE particle is

$$p_i = \frac{n_i}{N_i} \tag{7}$$

The total proportion of HDPE particle in all samples is

$$p = \frac{\sum_{i=1}^m n_i}{\sum_{i=1}^m N_i} \tag{8}$$

Then the deviation of sample i is

$$X_i = \frac{p_i}{p} \tag{9}$$

Calculate its average value and standard deviation:

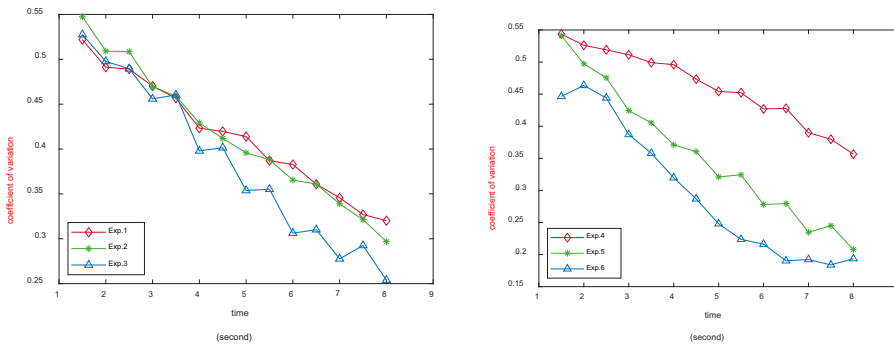
$$\bar{X} = \frac{\sum_{i=1}^m X_i}{m} \tag{10}$$

$$S = \sqrt{\frac{\sum_{i=1}^m (X_i - \bar{X})^2}{m-1}} \tag{11}$$

Then the variation coefficient C_V is expressed as

$$C_v = \frac{S}{\bar{X}} \tag{12}$$

Through sample data extraction and processing, the curves of HDPE particle's variation coefficient with time in nine experiments are shown in figure 9.



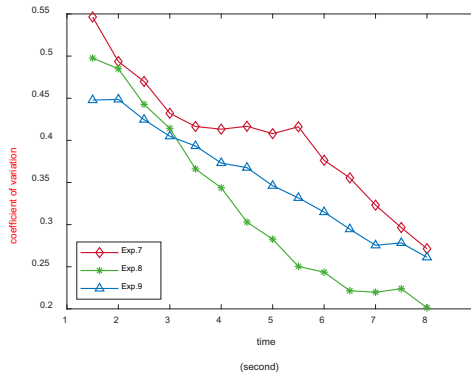


Fig. 9. The curve of variation coefficient.

4.2 Analysis of orthogonal experiment results

At an interval of 1s, the variation coefficients of all experiments are shown in table 5.

Table 5. The coefficient of variation.

| time(s) | Exp.1 | Exp.2 | Exp.3 | Exp.4 | Exp.5 | Exp.6 | Exp.7 | Exp.8 | Exp.9 |
|---------|--------|--------|--------|--------|--------|--------|--------|--------|--------|
| 1 | 0.5348 | 0.5870 | 0.5559 | — | — | — | — | 0.5291 | — |
| 2 | 0.4912 | 0.5092 | 0.4977 | 0.5262 | 0.4974 | 0.4636 | 0.4936 | 0.4849 | 0.4486 |
| 3 | 0.4702 | 0.4694 | 0.4559 | 0.5114 | 0.4244 | 0.3871 | 0.4322 | 0.4143 | 0.4049 |
| 4 | 0.4232 | 0.4290 | 0.3979 | 0.4960 | 0.3711 | 0.3198 | 0.4133 | 0.3437 | 0.3731 |
| 5 | 0.4139 | 0.3958 | 0.3538 | 0.4543 | 0.3210 | 0.2480 | 0.4080 | 0.2827 | 0.3462 |
| 6 | 0.3828 | 0.3654 | 0.3062 | 0.4269 | 0.2780 | 0.2163 | 0.3763 | 0.2436 | 0.3149 |
| 7 | 0.3457 | 0.3390 | 0.2777 | 0.3898 | 0.2348 | 0.1923 | 0.3231 | 0.2197 | 0.2755 |
| 8 | 0.3202 | 0.2969 | 0.2539 | 0.3566 | 0.2077 | 0.1936 | 0.2714 | 0.2013 | 0.2612 |

For the three factors, the average value of the final variation coefficient at 8s when taking each level value is calculated respectively. The smaller the average variation coefficient, The better the level value. Thus, the optimal level of intersection angle of side blades is 45 °, whose average variation coefficient k_{amin} equals to 0.2446. The optimal level of circumferential distribution angle is 120 °, whose average variation coefficient k_{bmin} equals to 0.2352. The optimal level of axial distribution spacing is 164mm with average variation coefficient k_{cmin} equivalent to 0.2384.

Perform range analysis. The ranges of k_a , k_b and k_c are 0.0457, 0.0809 and 0.0665 respectively. Therefore, the order of importance of the three factors is circumferential distribution angle, axial distribution spacing and then intersection angle of side blades.

According to the above, the theoretical optimal level combination is 3-2-1, which is the same as the conditions of Exp. 8. However, the variation coefficient of Exp. 6 is even lower than that of Exp. 8. Therefore, in terms of the current orthogonal experiment, the actual optimal level combination is 2-3-1, which represents that the intersection angle of side blades is 40 °, the circumferential distribution angle is 180 °, and the axial distribution spacing is 164mm.

5 Verification of strength and abrasion resistance

For Exp.6, check the pressure on ploughshares and the resistance moment on the main shaft. Process the force data derived from EDEM, then the results are shown in figure 10.

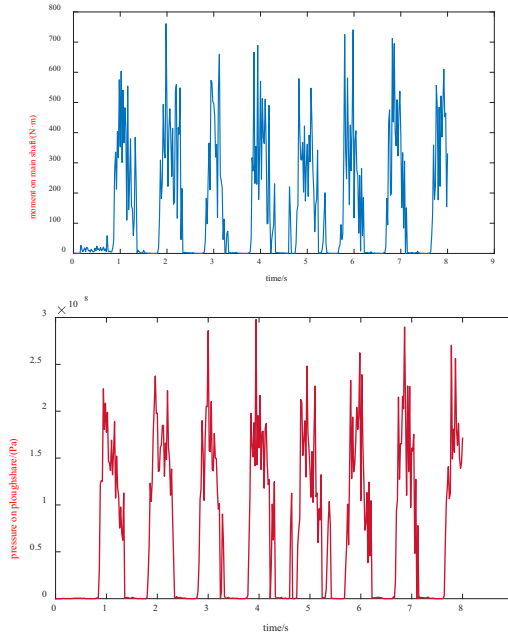


Fig. 10. Curve of resistance moment and pressure of Exp. 6.

At 1.02s in the start-up stage, the resistance moment of the main shaft subjected to the granular material is $603.5\text{N}\cdot\text{m}$. And the maximum resistance torque is $760.8\text{N}\cdot\text{m}$ at 1.98s. The magnitude of the resistance moment is close to the results by empirical formula ^[13] in industrial practice, which confirms the rationality and accuracy of the simulation.

At 3.94s, the maximum pressure on the ploughshare is 298MPa, which lasts extremely short. In general, the average pressure is approximately 200MPa, lower than the yield stiffness of stainless steel. Therefore, the abrasion resistance and strength of the mixing structure are considered as acceptable.

6 Conclusion

Based on the discrete element method, the simulation model of ploughshare mixer and plastic particles is established, and three parameters are studied by orthogonal experiment. The optimal result is from the sixth experiment when the intersection angle of side blades is 40° , the circumferential distribution angle is 180° , and the axial distribution spacing is 164mm. And its strength and abrasion resistance are verified as acceptable.

References

1. Haoran Xu, Fuqiang He, Yajun Xue, et al. Study on structural optimization design and characteristics of multifunctional wood plate double screw mixer based on EDEM [J]. Mechanical strength, 2021, 43 (02): 366-372.

2. Ke Zhang, Shuo Zhang, Yu Wenda, et al. Spiral numerical simulation analysis based on discrete element-finite element coupling simulation[J]. Journal of Shenyang Architecture University (natural science edition), 2021, 37 (04): 746-752.
3. Laurent B F C, Cleary P W. Comparative study by PEPT and DEM for flow and mixing in a ploughshare mixer [J]. Powder technology, 2012, 228: 171-186.
4. Cleary P W. Particulate mixing in a plough share mixer using DEM with realistic shaped particles [J]. Powder technology, 2013, 248: 103-120.
5. Alian M, Ein-Mozaffari F, Upreti S R. Analysis of the mixing of solid particles in a plowshare mixer via discrete element method (DEM)[J]. Powder Technology, 2015, 274: 77-87.
6. Bo Peng, Qin Xiao. New powder mixing equipment used in China's fine chemical industry in recent years [J]. Progress in chemical industry, 1995 (06): 34-37.
7. Wangchang Li, Yao Zhang. Progress of high-efficiency powder mixer [J]. Zhejiang chemical industry, 1997 (01): 8-12.
8. Yilun Wu, Jie Feng. Material mixing process in plough mixer [J]. Fire control technology and product information, 2005 (06): 19-23.
9. Fang Z, Peng S, Yi J, et al. Structure optimization of plough blades in a ploughshare mixer using the DEM simulations[J]. Engineering Computations, 2020.
10. Guoming Hu. Discrete element method analysis and Simulation of granular system: industrial application of discrete element method and brief introduction of EDEM software [M]. Wuhan: Wuhan University of Technology Press, 2010.
11. Shaohua Li, Mingliang Zhu, Lidong Zhang, et al. Analysis of radial mixing evaluation method of three component particles in rotary device [J]. Progress in chemical industry, 2013, 32 (06): 1224-1229.
12. Ya Mao, Xiong fan, Zhi Jiang. Study on mixing characteristics of vertical continuous mixer based on EDEM [J]. Computer simulation, 2018, 35 (12): 181-184.
13. Zhiping Chen, Xuwen Zhang, Xinghua Lin, et al. Design and selection manual of stirring and mixing equipment[M]. Beijing: Chemical Industry Press, 2004.